Int. J. Electrochem. Sci., 6 **(2011)** 2122 - 2130

International Journal of
ELECTROCHEMICAL
SCIENCE
www.electrochemsci.org

Photovoltaic Performance of New-Structure ZnO-nanorod Dye-Sensitized Solar Cells

M. H. Lai[1], *M. W. Lee*[1,*] , *Gou-Jen Wang*[2] *and M. F. Tai*[3]

[1]Institute of Nanoscience and Department of Physics, National Chung Hsing University, Taichung, 402, Taiwan
[2]Department of Mechanical Engineering and Institute of Biomedical Engineering, National Chung Hsing University, Taichung, 402, Taiwan
[3]Department of Physics, National Tsing Hua University, Hsinchu, 30013, Taiwan
[*]E-mail: mwl@phys.nchu.edu.tw

Received: 14 April 2011 / *Accepted:* 12 May 2011 / *Published:* 1 June 2011

Currently, the photoelectrode of nanorod-based dye-sensitized solar cells (DSSCs) consists of nanorods grown on a transparent conducting layer (TCO) substrate. This work presents a new structure for nanorod DSSCs. ZnO nanorods and a ZnO film were cogrown using a one-step chemical-vapor deposition method. The ZnO film functioned as the TCO of the DSSC. The ZnO nanorod/ZnO film structure was sensitized with D149 or N719 dye and assembled into a DSSC. Two notable features in this new DSSC structure are: (1) the junction between the TCO film and the nanorods is completely eliminated; (2) the TCO and the photoelectrode are made of the same material. Testing showed that under AM1.5 illumination, a short current density of 15.7 mA/cm^2 and a power conversion efficiency η of 1.82% can be achieved. The η is more than two times higher than the η reported earlier for ZnO-nanorod DSSCs with the same structure.

Keywords: zinc oxide, nanorod, dye-sensitized, solar cell

1. INTRODUCTION

Dye-sensitized solar cells (DSSCs) are a promising low-cost alternative to silicon-based photovoltaic solar cells [1].The key component of a DSSC is a photoanode comprised of a film of sintered oxide semiconductor nanoparticles (TiO_2) coated onto a transparent conducting oxide (TCO, usually fluorine-doped tin oxide-FTO) substrate [2]. The high efficiency of DSSCs can be attributed to their three-dimensional nanoporous nanoparticle architecture, which greatly increases the surface area for dye adsorption, resulting in enhanced light absorption and high power conversion efficiency. An efficiency of 11.3% was achieved in 2005 [3]. However, further improvement in efficiency has been

slow over the last decade. One problem is that not all of the photogenerated electrons can reach the collecting electrode. Electron transport within the nanoparticle network occurs via a series of hops (or trapping /detrapping) to neighboring particles. It has been estimated that a photoexcited electron undergoes 10^3 – 10^6 trapping/detrapping events before it reaches the collecting electrode [4].This trapping process leads to increased scattering and slows down the electron transport, which increases the recombination of the electrons with the oxidized dye molecules or the oxidized redox species, hence, reducing efficiency.

A promising strategy for improving electron transport in DSSCs is to replace the nanoparticle photoelectrode with single-crystalline nanorod (or nanowire, nanotube) photoelectrodes. Electrons can be conducted through a direct electron path within a nanorod, instead of by multiple-scattering transport between nanoparticles. Much work has been performed on the synthesis of TiO_2, ZnO and CdSe nanorods for applications in DSSCs [5-8]. Experiments reveal that electron transport is tens to hundreds times faster in nanorod-based DSSCs than in nanoparticle DSSCs [9,10]. Currently, nanorod arrays are grown on an FTO glass substrate but there is a disadvantage to this structure - the photoelectrode and the TCO layer are made of different materials and a heterogeneous interface exists between them. This interface forms a source for electron scattering. Chen *et al*. recently demonstrated a novel DSSC design, growing ZnO nanorods on the top of a ZnO film [11].The ZnO film replaces the FTO layer as the TCO layer. ZnO is a good TCO material because it has an energy gap of E_g = 3.4 eV, hence, is transparent in the visible spectral range. Their structure was grown by a two-step process: a Ga-doped ZnO film was first grown on a substrate, after which ZnO nanorods were grown on top of the film. This structure eliminated the heterojunction between the TCO film and the nanorods. A power conversion efficiency of 0.77% was achieved by Chen *et al*.

In an earlier work we fabricated Chen's new-structure DSSCs using a method simpler than Chen's method [12]. A one-step method was used to grow ZnO nanorods and a ZnO film. A power conversion efficiency of 0.73% was achieved. In this work we improved the one-step growth and fabrication of the solar cells. Investigation of the photovolatic properties of the ZnO-nanorod DSSCs showed the new DSSCs to yield efficiencies much higher than those of Chen's and our earlier new-structure ZnO-nanorod DSSCs. There are two notable features in this new DSSC structure: (1) the junction between the TCO film and the nanorods is completely eliminated; (2) the TCO and the photoelectrode are made of the same material, hence, electron conduction and power conversion efficiency are expected to improve.

2. EXPERIMENTAL

2.1. Growth of ZnO nanorods and ZnO films

ZnO nanorods and a ZnO film were cogrown by a one-step catalyst-free chemical-vapor-deposition (CVD) method [12]. Single-crystalline c-plane (0001) sapphire substrates were loaded into an alumina boat, which was then placed inside a one-inch quartz tube in a horizontal tube furnace. The substrate was placed 7-11 cm downstream from the Zn source material. The furnace was heated to

870˚C at a heating rate of 12 ˚C/min and then maintained at the heated temperature for 40 min. Ar and O_2 gases were fed into the quartz tube at flow rates of 16.4 sccm (Ar) and 1.8 sccm (O_2). During the first growth stage, a ZnO film grew on the substrate. In the second growth stage, ZnO nanorods were grown on top of the ZnO film.

2.2. Fabrication of solar cells

For fabrication of DSSCs, the grown ZnO nanorods were immersed in a 60˚C, 0.5 mM D149 dye (Mitsubishi paper) solution (a mixture of 1mM chenodeoxycholic acid in tert-butyl alcohol and acetonitrile, 1:1 volume ratio) for 8h. We also investigated the performance of the cells sensitized with the commonly used dye-N719 (0.3 mM). An FTO glass with a 150 μm-thick Pt foil attached to it was used as the counterelectrode. The photoanode and the counterelectrode were assembled into a solar cell using a 25μm-thick surlyn spacer. The electrolyte was composed of 0.5M LiI, 0.05M I_2, 0.5M 4-tert-butylpyridine, and 0.6M butylmethylimidazolium iodide in acetonitrile and valeronitrile. The electrolyte was injected into the cell through two predrilled holes (size 1 mm) on the counterelectrode. The active area of the cell, limited by the size of the grown sample, was ~ 2 mm×2 mm. Photovolatic measurements

The current- voltage (*I-V*) curves were recorded with a keithley 2400 source meter. The light source was a 150W xenon lamp (Oriel) with an Oriel filter to simulate the AM1.5 solar spectrum. A metal mask of dimension 2.5 mm×2.5 mm was placed above the solar cell during the measurement. The external quantum efficiency (EQE) spectra were measured using a monochromator (Acton) with a 250W tungsten halogen lamp.

2.3. Growth of ZnO nanorods for conventional DSSCs

For comparison, a reference solar cell that had the structure of conventional DSSCs - ZnO nanorods grown on an FTO glass substrate - was grown by the chemical bath deposition (CBD) method. Prior to the growth, a seed layer of ZnO nanoparticles was first deposited by immersing an FTO substrate into a solution of 0.5 M zinc acetate $Zn(CH_3COO)_2 \cdot 2H_2O$ and hexamethylenetetramine $C_6H_{12}N_4$ (HMT) for 30 min. ZnO nanorods were then grown by immersing the seed-coated substrate into a beaker containing a 95˚C, 0.01 M solution of zinc nitrate hexahydrate and HMT for 5 h. The process was repeated five times to obtain higher density and longer nanorods.

3. RESULTS AND DISCUSSION

Figure 1(a) shows a field-emission transmission electron microscopic (FESEM) cross-sectional image of the ZnO nanorods grown by the one-step CVD process. The nanorods have diameters in the range of 150 - 220 nm and lengths of ~ 12 μm. A layer of ZnO film (thickness ~ 2.5 μm) can be clearly seen in the picture. The diameter and film thickness of the nanorods are found to decrease as the O_2

flow rate was increased. The nanorods are roughly perpendicular (angle 60-90º) to the ZnO film. Figures 1 (b) and (c) show a TEM image of a single nanorod and its electron diffraction pattern, which reveals the single-crystalline quality of the nanorod.

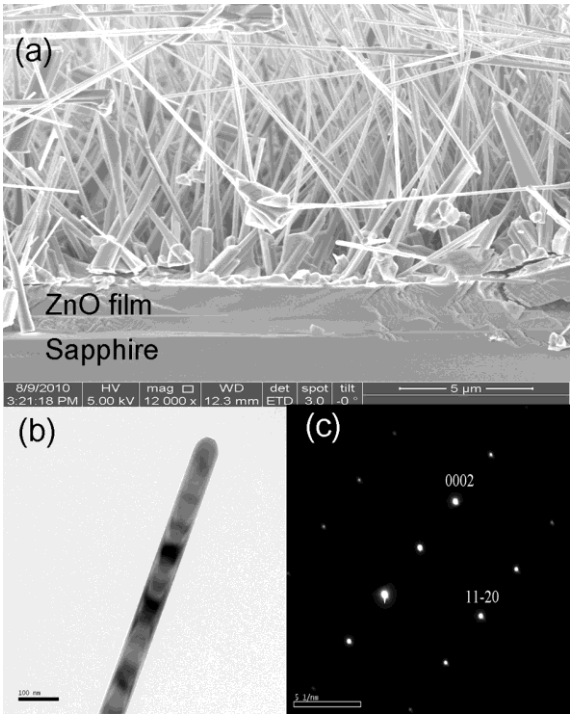

Figure 1 (a) FESEM image of ZnO nanorods on top of a ZnO film. (b) TEM image of a single ZnO nanorod. (c) Electron diffraction pattern of a single nanorod.

The X-ray diffraction pattern, shown in figure 2, reveals that the nanorods are of the wurtzite structure with lattice constants of a = 3.176 Å, c = 5.187 Å.

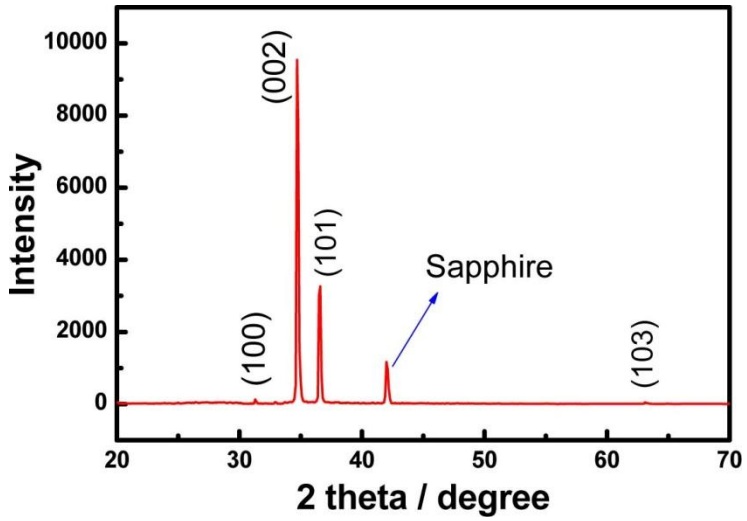

Figure 2. X-ray diffraction pattern of the ZnO nanorods.

The most pronounced diffraction peak is (002), indicating that the preferred direction of growth for the nanorods is along the *c* axis. Figure 3(a) depicts the schematic diagram of a new-structure ZnO nanorod DSSC fabricated on sapphire. For comparison, the diagram of a conventional ZnO nanorod DSSC, fabricated on a FTO glass substrate, is also shown in figure 3(b).

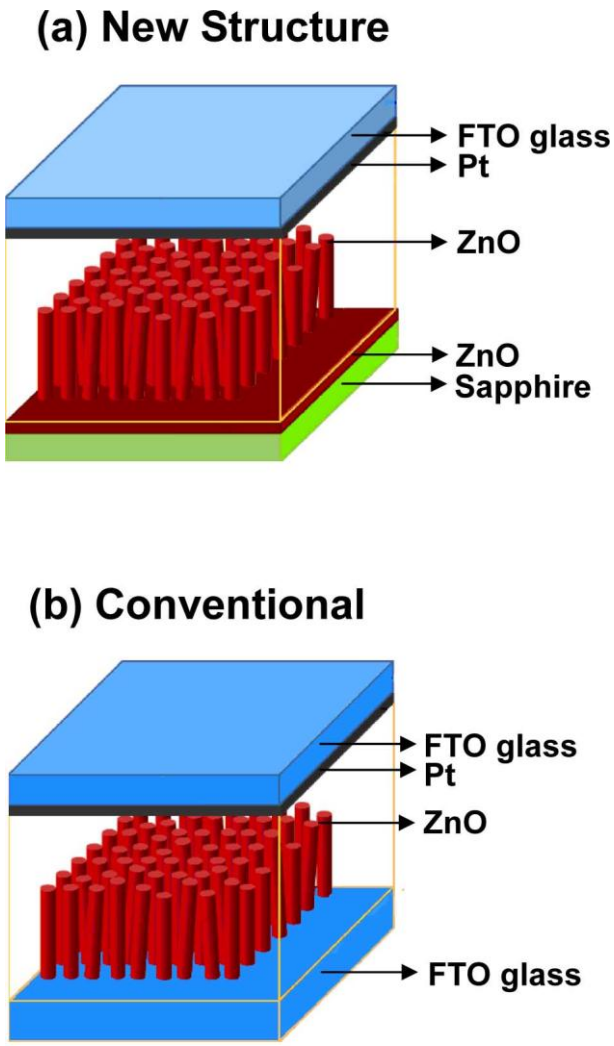

Figure 3. Schematic diagrams of the (a) new-structure ZnO nanorod DSSC fabricated on sapphire. (b) Conventional ZnO nanorod DSSC fabricated on a FTO glass substrate.

Figure 4(a) shows typical *I-V* curves of the new-structure and conventional-structure ZnO-nanorod DSSCs under AM1.5 (100 mW/cm^2) illumination. The inset shows the dark *I-V* curve of the new-structure DSSC (note that the dark currents are extremely small, ~10^{-3} mA/cm^2 over the voltage range from 0-0.4 V. Small dark currents are advantageous to the performance of DSSCs). The summarized photovoltaic parameters for the five new-structure DSSCs (sample Nos. 1-5) are listed in table 1. The best DSSC has a short-circuit current density of J_{sc} = 15.7 mA/cm^2, an open-circuit voltage of V_{oc} = 0.55 V, a fill factor = 21% and a power conversion efficiency of η = 1.82%. The data are very consistent among various samples. Moreover, different dyes (D149, N719) yield nearly the same η. In

comparison, the conventional DSSC (sample No. 6) yields a short-circuit current density of J_{sc} = 5.51 mA/cm^2 and an efficiency of η = 1.37%.

Table 1. Photovoltaic performance of five new-structure (Nos. 1-5) and one conventional-structure (No. 6) ZnO-nanorod solar cells.

	Sample no.	J_{sc} (mA/cm^2)	V_{oc} (V)	FF (%)	η (%)	Dye
New structure	1	15.7	0.55	21.1	1.82	D149
	2	15.6	0.54	21.5	1.81	D149
	3	15.5	0.54	21.3	1.78	N719
	4	15.6	0.50	19.6	1.53	N719
	5	15.4	0.51	20.1	1.59	N719
Conventional structure	6	5.51	0.65	38.2	1.37	N719

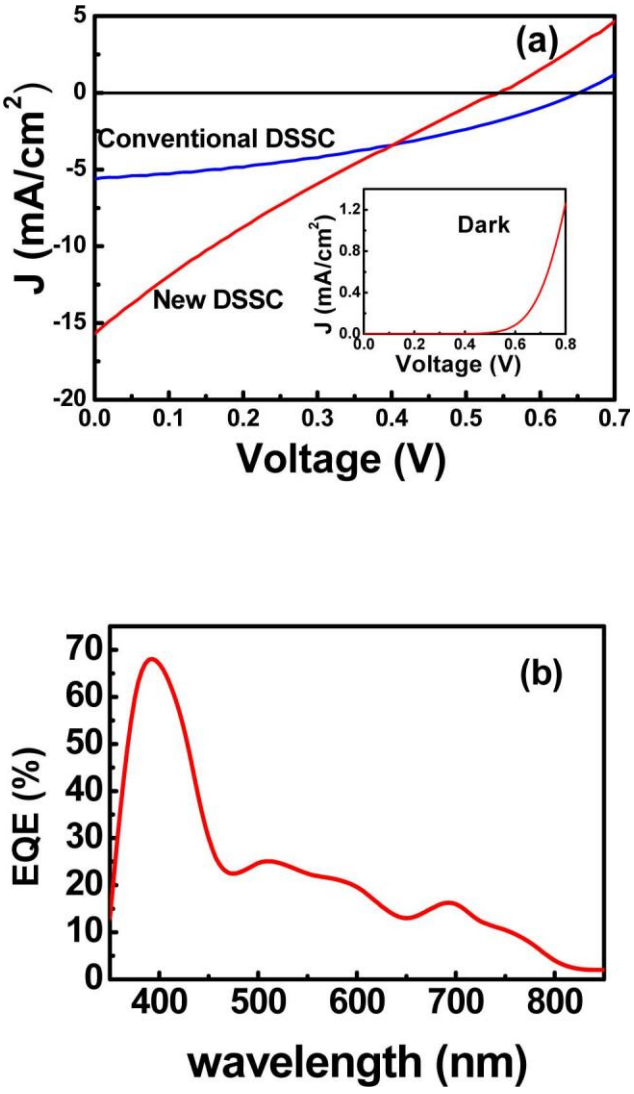

Figure 4. (a) *I-V* curves of the ZnO-nanorod DSSC. (b) EQE curve of the new-structure ZnO DSSC.

Figure 4(b) displays the EQE spectrum of the ZnO-nanorod DSSC (N719 dye). The strong peak at 390 nm and the broad peak at 500-600 nm are attributed to the characteristic excitations of the N719 dye. The pronounced peak at 390 nm also includes the contribution from the fundamental absorption edge (valence band to conduction band) of ZnO nanorods. An interesting feature of the new DSSC structure is that the ZnO film also contributes to light absorption in the ultraviolet spectral range (390nm). Thus, the ZnO film serves both as the TCO layer and as a light absorber. In contrast, the FTO layer in a conventional DSSC only functions as a TCO layer.Conventional ZnO-nanorod DSSCs typically have efficiencies of η ~1.0-2.0% [13,14]. The η = 1.82% obtained in the present work is nearly equal to that of the best conventional DSSCs. Moreover, the η is more than two times larger than the η = 0.77% (Chen's result) and 0.73% (our previous result) from the new structure DSSCs [11,12]. The significant enhancement in η indicates that the new structure is a feasible concept for fabricating high-performance DSSCs. With further improvement in the fabrication process, we expect the new structure DSSCs to yield efficiencies exceeding the best conventional nanorod DSSCs soon.

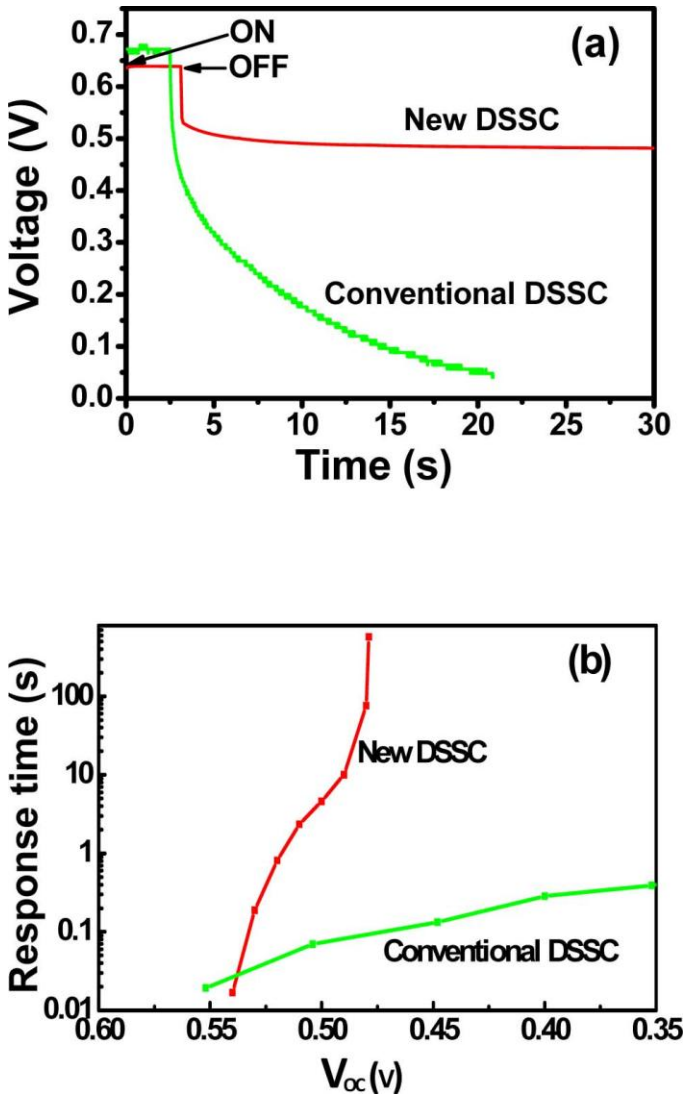

Figure 5. (a) Open-circuit voltage decays for the new and conventional ZnO-nanorod DSSCs. (b) Response time as a function of V_{oc}.

The enhanced efficiency in the new-structure DSSC can be attributed to the junctionlessness and the same TCO/nanorod-material design of the new electrode structure. Insight into the enhancement in performance can be obtained by investigating the photoelectron lifetimes using the open-circuit voltage-decay measurements. Figure 5(a) shows open-circuit voltage-decay curves for the new and conventional-structure ZnO nanorod DSSCs after the illumination was turned off. The response time τ can be deduced from the derivative of the V_{oc} decay curve using the equation [15]:

$$\tau = -\frac{k_B T}{e}\left(\frac{dV_{oc}}{dt}\right)^{-1}$$

where k_B is the Boltzmann's constant, e is the elementary charge and T is the temperature. The calculated response times τ as a function of V_{oc} for the two types of DSSCs are displayed in figure 5 (b).

The response time increases with deceasing V_{oc}. It can be seen that the response time of the new-structure DSSC is much larger than that of the conventional DSSC. For example, τ = 4.5 s (new) at V_{oc} = 0.50 V, as compared to τ = 0.072 s (conventional). The enhancement in τ may be attributed to a reduction in carrier recombination. The V_{oc}–dependent response time is related to the charge transport of three types of carriers: the high V_{oc} region is related to electrons in the conduction band, the medium V_{oc} region is related to the bulk traps, and the low V_{oc} region is related to the surface traps [15]. The τ vs. V_{oc} curve for the new DSSC, shown in figure 5(b), belongs to the high V_{oc} region. Thus, it describes the lifetime of the electrons in the conduction band, which, in the present system, corresponds to the transport of free electrons within the ZnO nanorods and the ZnO film. A larger τ results in an increased carrier diffusion length, which leads to a larger photocurrent and an enhanced efficiency. The results indicate that the new photoanode structure greatly improves the carrier transport in solar cells.

4. CONCLUSION

In summary, we have demonstrated the growth of ZnO nanorods/ZnO film on a sapphire substrate using the CVD method. The new DSSC structure eliminates the junction between the TCO layer and the nanorod. The fabricated DSSCs yield power conversion efficiencies two times larger than that of the DSSCs in the previous work.

ACKNOWLEDGMENTS
The authors would like to thank the National Science Council of the Republic of China for financially supporting this research.

References

1. B. O'Regan and M. Grätzel, *Nature*, 353 (1991) 737.
2. D. Wei and G. Amaratumga, *Int. J. Electrochem. Sci*., 2 (2007) 897.

3. M.K. Nazeeruddin, F.D. Angelis, S. Fantacci, A. Selloni, G. Viscardi, P. Liska, S. Ito, B. Takeru and M. Grätzel, *J. Am. Chem. Soc.*, 127 (2005) 16835.
4. K.D. Benkstein, N. Kopidakis, J. van de Lagemaat and A.J. Frank, *J. Phys. Chem.* B, 107 (2003) 7759.
5. M. Adachi, Y. Murata, T. Okada and Y. Yoshikawa, *J. Electrochem. Soc*., 150 (2003) G488.
6. M. Dürr, A. Schmid, M. Obermaier, S. Rosselli, A. Yasuda and G. Nelles, *Nat. Mater*., 4 (2005) 607.
7. J. Baxter and E.S. Aydil, *Appl. Phys. Lett*., 86 (2005) 053114.
8. D. Soundararajan, J.K. Yoon, Y.I. Kim, J.S. Kwon, C.W. Park, S.H. Kim and J.M. Ko, *Int. J. Electrochem. Sci*., 4 (2009) 1628.
9. G.K. Mor, K. Shankar, M. Paulose, O.K. Varghese and C.A. Grimes, *Nano Lett*, 6 (2006) 215.
10. K. Zhu, N.R. Neale, A. Miedaner and A.J. Frank, *Nano Lett*, 7 (2007) 69.
11. H. Chen, A. Du Pasquier, G. Saraf, J. Zhong and Y. Lu, *Semicon. Sci. and Tech*., 23 (2008) 045004.
12. M.H. Lai, A. Tubtimtae, M.W. Lee, G. J. Wang, *Int. J. Photoenergy*, Vol. 2010 Article ID: 497095 DOI: 10.1155/2010/497095.
13. C.Y. Jiang, X.W. Sun, G.Q. Lo and D.L. Kwong, *Appl. Phys. Lett*., 90 (2007) 263501.
14. M. Guo, P. Diao, X. Wang and S. Cai, Appl. Surf. Sci., 249 (2005) 71.
15. J. Bisquert, A. Zaban, M. Greenstein and I. Mora-Seró, *J. Am. Chem. Soc*., 126 (2004) 13550.